research reviews

Transparent, flexible electrodes and sensors based on carbon nanotube thin films

Jordi Pérez-Puigdemont[1]*, Nuria Ferrer-Anglada[1,2], Bernat Terrés[1,2], Martti Kaempgen[2], Siegmar Roth[2]

1. Departament de Física Aplicada, Universitat Politècnica de Catalunya
2. Max-Planck-Institut für Festkörperforschung, Stuttgart, Germany

Resum

Hem obtingut capes primes de Nanotubs de Carboni d'una sola paret (CNT) sobre un substrat amb un mètode molt simple, que poden ser emprades com elèctrodes flexibles i transparents en dispositius electrònics. Per tal d'obtenir dispositius reproduïbles amb propietats similars, en particular amb similar impedància $Z(\omega)$, és important relacionar les propietats elèctriques amb la quantitat de CNTs presents en la capa.

Per això, hem realitzat capes primes de CNTs sobre substrats flexibles i transparents (PPC, policarbonat de propilè) amb diferents densitats de CNT. A partir d'un mètode iteratiu matemàtic i de l'Anàlisi Tèrmogravimètric (TGA) de cada mostra, hem pogut determinar la quantitat de CNTs presents en cada mostra. També n'hem fet una estimació a partir de l'espectroscòpia d'absorció òptica. Hem vist que els dos mètodes donen resultats coherents. Hem analitzat les diferents mostres mesurant la impedància elèctrica a diferents freqüències, fins 110 MHz. Les capes primes amb poca densitat de CNTs són semiconductores, en canvi les denses són metàl·liques, i prou conductores per ser utilitzades com elèctrode de treball en un procés electroquímic. Podem obtenir així composites CNT-polímer conductor o CNT-metall, electroquímicament.

Amb l'objectiu de les aplicacions per a sensors, utilitzant les capes primes de CNT com elèctrode de treball hem obtingut composites CNT-polímer conductor, depositant-hi electroquímicament un polímer conductor, polipirrol o polianilina. Hem analitzat les propietats del dispositiu com a sensor electroquímic, observant la seva resposta en funció del pH, mesurant el potencial en circuit obert en funció del pH de la solució, entre 1 i 13. Els resultats mostren una bona sensibilitat, linearitat i estabilitat. Per això, els dispositius CNT/polipirrol i CNT/polianilina poden tenir aplicacions com a sensors o biosensors en estat sòlid, depositats sobre qualsevol superfície de forma arbitrària, que pot ser transparent i flexible.

Paraules clau: nanotubs de carboni · elèctrodes transparents i flexibles · sensors flexibles · capes primes

Abstract

We obtained thin films of single-walled carbon nanotubes (CNTs), which may be used as transparent, flexible electrodes in electronic devices, on a substrate using a very simple method. In order to construct reproducible devices with similar properties, in particular with similar impedance $Z(\omega)$, it is important to associate the electrical properties with the number of CNTs in a network. We prepared thin CNT networks on transparent, flexible substrates (PPC, polypropylene carbonate) with different CNT densities. The number of CNTs was estimated using a mathematical method based on the data obtained from thermo-gravimetric analysis (TGA). We were able to estimate the relative number of CNTs using optical absorption spectroscopy. These two methods are in good agreement. We also analysed the various samples using electrical impedance measurements at frequencies of up to 110 MHz. Low-density networks are semiconductors, whilst high-density networks behave like metals and are sufficiently good conductors to be used as working electrodes in electrochemical processes. It is thus possible to obtain CNT polymer and metal composite conductors electrochemically.

With sensor applications in mind, we used CNT thin films as a working electrode to obtain a composite CNT-conducting polymer. This was performed by electrochemically depositing a conducting polymer — polypyrrole or polyaniline — on the electrode. The pH dependence of the device was measured by recording its open circuit potential in various buffer solutions. This enabled us to analyse the properties of the device as an electrochemical sensor. The results showed a good sensitivity, linearity and stability in both cases. Thus, the CNT/polypyrrole and CNT/polyaniline devices could have applications as solid-state gas sensors or biosensors when they are deposited on transparent and flexible surfaces of any shape.

Keywords: carbon nanotubes · transparent and flexible electrodes · flexible sensors · thin films

* Author for correspondence: Jordi Pérez-Puigdemont. Departament de Física Aplicada, Universitat Politècnica de Catalunya. Jordi Girona 3-5, E- 08034 Barcelona, Catalonia, EU. Tel. +34 934017761. Fax +34 934016090. E-mail: jordi.perez@fa.upc.edu

1. Introduction

Carbon nanotubes (CNTs) were discovered in 1991 by Iijima [1]. More than 17 years after their discovery, they are still one of the hottest research areas in the fields of materials science and engineering. This interest is driven by their singular mechanical, electrical and thermal properties [2-4] and, more importantly, by their possible applications [5-11]: field emission-based flat panel displays; transistors; quantum wires; hydrogen storage devices; structural reinforcement agents; chemical and electrochemical sensors; and nanoscale actuators, probes, and tweezers. Some of these applications are based on a single nanotube (transistors, nano-actuators, sensors, and tweezers), and some on a bundle of CNTs (displays, actuators, sensors, optical modulators, flexible and transparent electrodes or transistors) [12-14]. Others are based on a composite whereby CNTs are used to reinforce a desired property of the host material for a specific application [15-18].

The low dimensionality and the highly regular structure of CNTs have provided fertile ground for theoretical physics, and specifically for solid state physics with regard to the dependence of a CNTs electronic properties on its chirality [2, 3, 19]. In addition, intrinsic quantum effects such as quantised conductance, Coulomb blockade, the Aharonov-Bohm effect and the Kondo effect are among those predicted by theoreticians and observed by experimentalists [19].

Our research focuses on single-wall carbon nanotube (SWCNTs) applications. The conductivity and high aspect ratio of SWCNTs are useful properties for producing transparent, flexible networks, which may be used in many different fields including sensors [20-22], flexible and transparent transistors [13, 23], and transparent electrodes [12, 24-25]. Moreover, these properties are useful for preparing composites, since an SWCNT network may be used as a working electrode to electrochemically grow a metal or a conducting polymer — polypyrrole (PPy) or polyaniline (PA) — on it. We prepared a CNT/PPy and a CNT/PA, which we characterised as pH sensors.

Single-walled carbon nanotubes have high conductivity and quasi-ballistic behaviour at room temperature [2-4]. Thus, when CNTs are deposited on an insulating transparent substrate, conductive, transparent films (T=80%-90%) in the visible-NIR range are achieved [12, 24]. These thin films may be used as transparent electrodes in organic electronic devices because they have greater mechanical flexibility than indium tin oxide. They are particularly well suited as electrodes in organic solar cells as they increase their performance [26]. In many cases (e.g. in solar cells) flexibility is the most important parameter for achieving good integration in the architectural structure of a building.

It has been reported that both conductance and the I(V) characteristics depend strongly on the number of CNTs deposited on the substrate and on the chemical treatment to which it is subjected [27, 28]. Several applications have been advanced for CNT thin films, or networks, on a substrate at different frequencies [29, 30].

2. Transparent electrodes

2.1. Experimental

The first step in building electrodes or pH sensors is to obtain a transparent, conductive network of nanotubes over the desired substrate. Several production methods are available: spray deposition, electric field deposition, dip coating and adsorption deposition. These methods are described in detail below.

2.1.1. Spray Deposition

The spray coating technique is the simplest and quickest method for depositing CNTs on a surface. Using a commercial airbrush (from Harder & Steenbeck, Germany), one can easily tune the transparency of the samples from 100 to 0%. After preparing a light suspension of CNT in sodium dodecyl sulphate (SDS), the suspension is directly sprayed onto the substrate without removing it from a heating plate. The temperature must be around 100 ºC (depending on the substrate) to accelerate the drying of the small droplets on the surface. This heating was extremely helpful when large surfaces were sprayed. In order to spread the carbon nanotubes as uniformly as possible, the formation of big droplets must be avoided, as they decrease the conductivity to transparency ratio of the samples. After the deposition step, the samples were immersed in de-ionised water to remove traces of SDS and dried with argon gas. Figure 1 shows the morphology of the resulting network observed using an AFM.

2.1.2. Electric field deposition

Electric field deposition is an easier and quicker way of coating transparent substrates with carbon nanotubes. Using two electrodes dipped into a CNT dispersion, this deposition technique runs automatically when a voltage is applied between them. The cathode may be of any sort of metal (copper in this case), but the anode electrode should be a layer of aluminium deposited on a transparent substrate (quartz glass).

Figure 2 shows the devices used in the procedure: the power supply, the electrodes and the CNT+SDS dispersion. Though carbon nanotubes are conductive or semi-conductive, they are
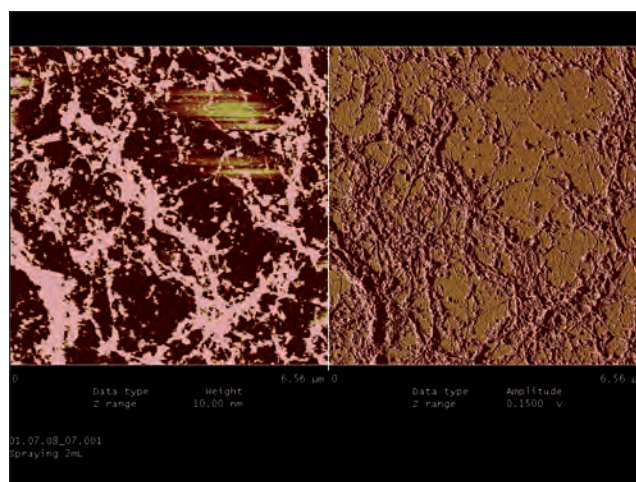

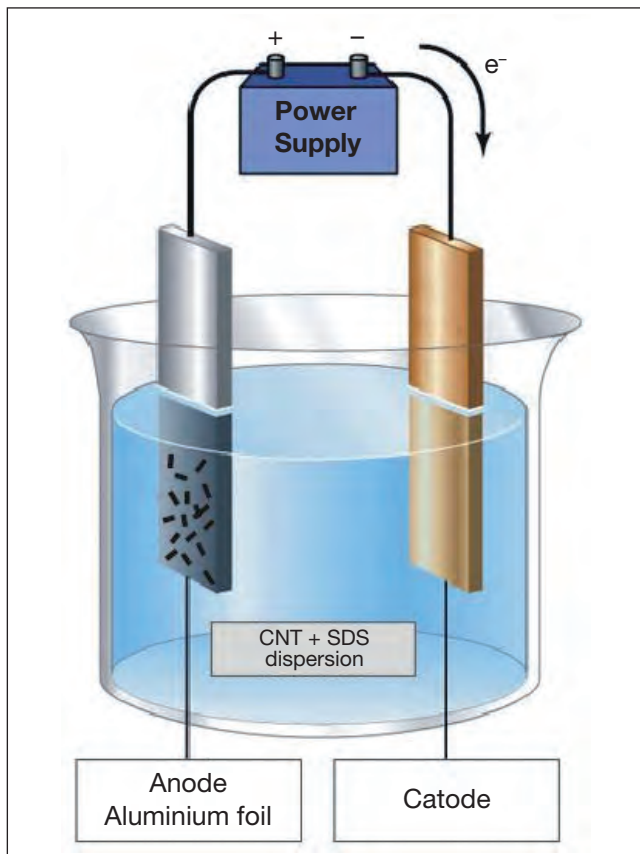Figure 1. Morphology of the CNT network after spray coating deposition.

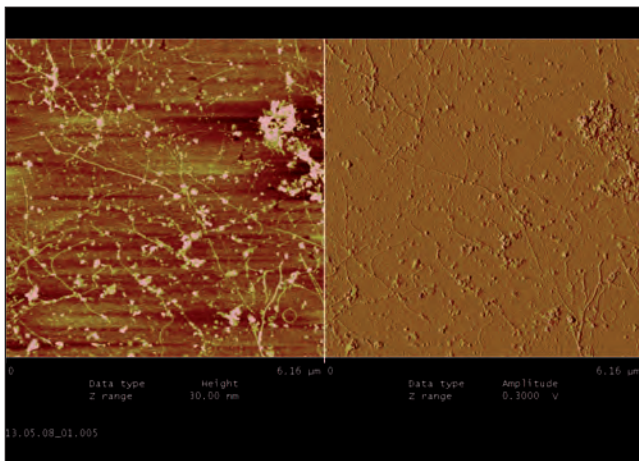Figure 2. Schematics of electric field deposition.

Figure 3. Morphology of the CNT network after electric field deposition.

electrically neutral. Under the effects of the electric field, therefore, the CNT may be oriented as a dipole but not moved towards the electrodes since the DC field between electrodes remains uniform.

The SDS plays an important role during the process as it assists motion of the CNTs. Although SDS molecules are also electrically neutral, once they have dissolved in de-ionised water the sodium cations (Na+) are delocalised and the SDS molecules become negatively charged. This negatively charged cap end becomes the hydrophilic part of the molecule that interacts with the oxygen elements of the H_2O molecule. The long CH_3 chain (hydrophobic part) remains electrically neutral and, by Van der

Waals interactions, tends to bundle with the CNT and the other SDS molecules. This behaviour is known as micelle formation.

The micelles (SDS+CNT) are negatively charged and are therefore attracted to the anode. The deposition on the anode takes place until the aluminium is completely oxidised and converted into aluminium oxide Al_2O_3. The aluminium oxide is transparent but is no longer conductive. This feature makes the process stop automatically when there is no more aluminium on the surface. By choosing the thickness of the layer, one can tune the concentration of the CNT on the surface. As a result, a CNT-based transparent, conductive layer is deposited on the glass substrate. Figure 3 shows the AFM image of the network obtained.

2.1.3. Dip coating deposition

The dip coating technique is a method whereby the substrate to be coated is immersed in a dispersion and then extracted at a well-defined extraction speed. The coating thickness is mainly defined by the extraction speed, the solid content and the viscosity of the liquid. The coating thickness can be calculated by the Landau-Levich [31] equation:

$$h = 0.94 \frac{(\eta \nu)^{2/3}}{\gamma^{1/6} (\rho g)^{1/2}} \quad (1)$$

By choosing the appropriate viscosity, the coating thickness can usually be varied but for CNT deposition we did not take these parameters into account. The substrates were coated several times in order to tune the concentration of the CNT on the surface. The more times the substrate is dipped into the dispersion, the greater the number of CNTs that adhere to the surface. The resulting network, deposited on a silicon oxide substrate, is shown as seen under an AFM in Figure 4.

2.1.4. Adsorption deposition

Adsorption deposition is comparable with dip coating deposition. In both methods, carbon nanotubes adhere to a surface by drying the dispersion. During adsorption coating, one drop of dispersion is deposited on a surface and afterwards blown away by an argon flow. The air flow direction is kept constant
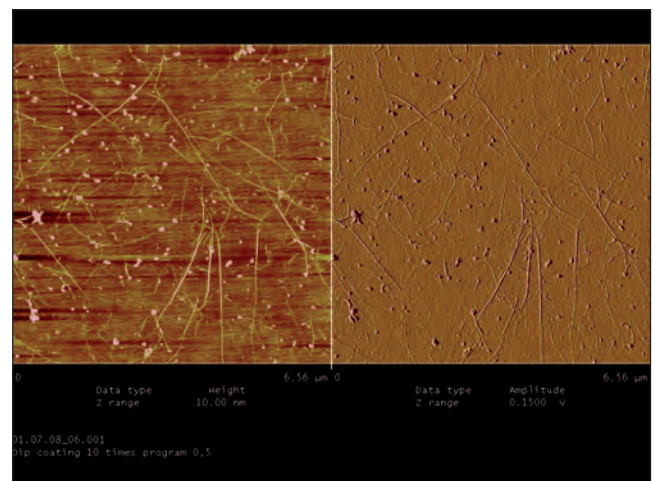

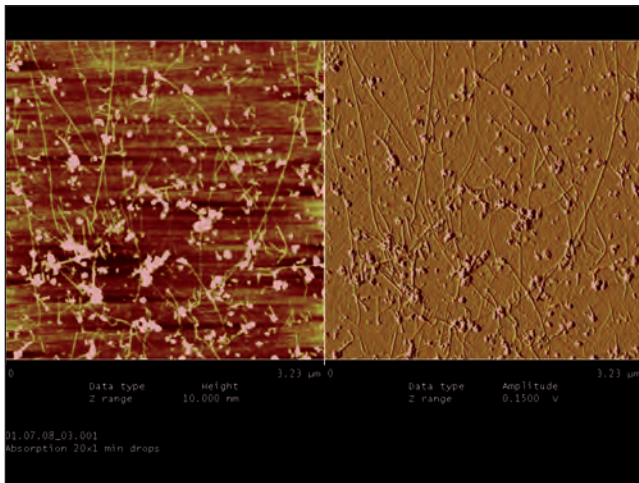Figure 4. CNT network on a silicon oxide substrate after the dip coating procedure.

Figure 5. AFM image of a CNT network after adsorption deposition (40 drops, slow dry).

for every drop. The direction in which the gas flows determines the orientation of the carbon nanotubes. Silicon oxide chips (4.5 mm x 4.5 mm) were used as a substrate to measure conductivity performance and quartz glass substrates (4.5 mm × 4.5 mm) to measure the transparency. The morphology is shown in an AFM image in Figure 5 (40 drops, slow dry).

2.2 Characterisation

2.2.1. TGA characterisation

A quantitative knowledge of the mass of SWCNTs deposited on a thin film is essential to achieving high reproducibility in SWCNT devices. Thermogravimetric analysis (TGA) in air and an easy optimisation algorithm were used to determine this quantity. The TGA of each thin film prepared shows that samples lose weight as the temperature is increased. For each sample, the TGA curve, $TGA_{Sample}(T)$, should be a weighted combination of the TGA curves of the substrate, $TGA_{Subs}(T)$, and the SWCNTs, $TGA_{SWCNT}(T)$. It is well known that PPC is completely pyrolysed between 250 and 300 ºC in a single step [32]. The curves, $TGA_{Subs}(T)$ and $TGA_{SWCNT}(T)$, both normalised to their maximum value, may be considered the basis of a certain geometric space in which the sample curves would be reconstructed.

First of all, an error equation was derived:

$$e^2 x, y = TGA_{Sample} T - xTGA_{Subs} T - yTGA_{SWCNT} T^2 \quad (2)$$

This defines the error surface (Figure 6). Finding its absolute minimum yields the weight proportion of the substrate and the SWCNTs, x_{min} and y_{min} , respectively. The minimum was determined using an adaptive gradient method. This method was selected due to its simple coding, reliability and low computational cost. The use of one algorithm or another should not vary the final results because the error surface only has one minimum value. This can easily be seen through the simple observation of the error surface.

The algorithm is controlled by a simple equation:

$$x_{n+1}, y_{n+1} = x_n, y_n - \mu_n \ e^2 x_n, y_n \quad (3)$$

which, when iterated, describes a path over the error surface from its starting point to the position of the absolute minimum (see Figure 6).

After a thousand-step process, Equation (2) reaches a position that is extremely close to the minimum position. To ensure that the algorithm reaches the absolute minimum, a random step over the (x, y) plane was performed after applying the gradient method.

When the weight proportions of the substrate and the SWCNTs had been calculated for the various samples using our method, they were seen to show a correlation. The correlation and the values of the points are correct because the points (x_{min}, y_{min}) are located on the line $y=1-x$, as can be seen in Figure 7. For the darkest sample, the SWCNT weight proportion calculated was the maximum value. However, a slight deviation from the theoretical line was observed and will be discussed below
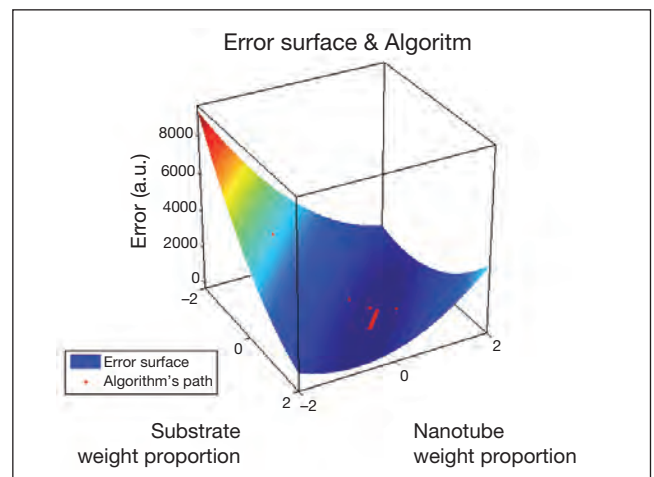

Figure 6. Surface of error and algorithm path over it. It can be seen that the surface of error has only one minimum.
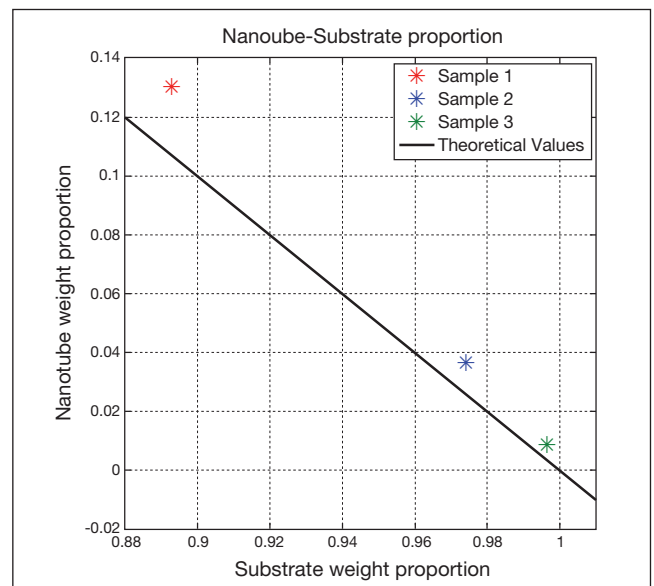

Figure 7. Calculated weight proportion values and theoretical values (y = 1 – x). They show good agreement; for the darkest sample, the calculated SWCNT weight proportion was the maximum possible value. The same was true of the other two samples.

2.2.2. AC-DC characterisation

The impedance measurement was performed using an Agilent 4294A precision impedance analyser in a range from 40 Hz to 110 MHz. The setup is shown in Figure 8.

It should be noted that we used the two-wire method due an easier impedance calibration: as SWCNT thin films exhibit high impedance, the contact resistance should be several orders of magnitude lower, and can therefore be rejected.

The analysis of the absolute impedance value in the frequency range observed gave us two major parameters: the low frequency impedance, which is the same as the DC resistance (R_{DC}), and the cutoff frequency (ω_0). These two values vary with the density of the SWCNTs in the thin film, namely, as the SWCNT density increases, the DC resistance decreases, while the cutoff increases proportionally to the density of the SWC-

NTs [33, 34]. This cutoff frequency is related to the mean distance between the junctions in the random nanotube network [34]. The impedance of the thin film starts to decrease at a constant rate above this frequency. This phenomenon is due to the fact that during a half period of the electric field, $T/2 < \pi/\omega_0$, the electrons do not have enough time to cross all the junctions on their way through the random nanotube network from one contact pad to another. As the frequency increases, the electrons cross fewer junctions, which act as potential barriers. As a result of this, the impedance decreases. Figure 9 shows the absolute value of the impedance for various samples. The cutoff frequencies for some samples are shown. This cutoff frequency is related to the TGA analysis.

Since the cutoff frequency and the DC resistance are related to the SWCNT density in the thin film, they must also be related to the SWCNT weight proportion that was calculated. This is shown in Figure 10 (note the correlation between the SWCNT weight proportions determined from TGA analysis and the DC resistance) and Figure 11, in which the correlation between the SWCNT weight proportion determined from TGA analysis and the cutoff frequency can be observed. For a sample with more tubes in the network, the distance between tube junctions is lower than in a sample with fewer tubes. Thus, the cutoff frequency for a dense sample is higher than the cutoff for a lighter sample.

2.2.3. Optical characterisation

In order to check the results obtained from the TGA analysis, we used the optical absorption spectra in the NIR range, as described in [35]. The peaks that appear from 5,000 cm^{-1} to 14,000 cm^{-1} are assigned to transitions across the Van Hove singularities in the electronic density of states of nanotubes, due to their one-dimensionality [36]. The second of these transitions,
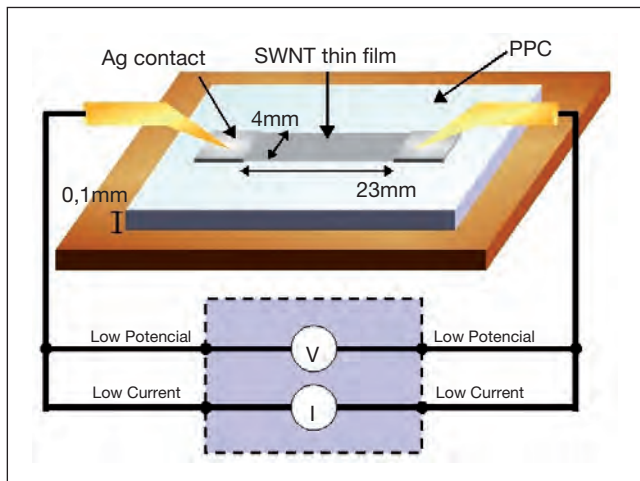

Figure 8. Impedance measurement setup. The two-wire method was chosen due an easier impedance calibration.
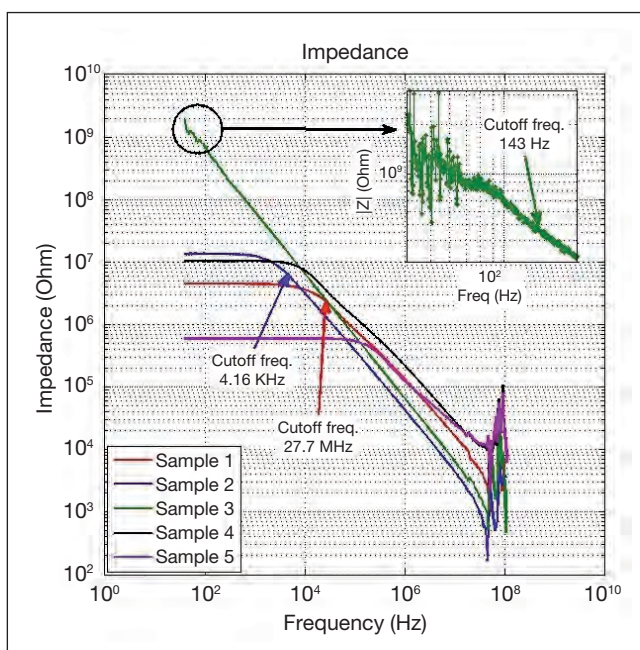

Figure 9. Absolute value of the impedance of various samples. The cutoff frequencies for some samples are shown. This cutoff frequency is related to the TGA analysis.
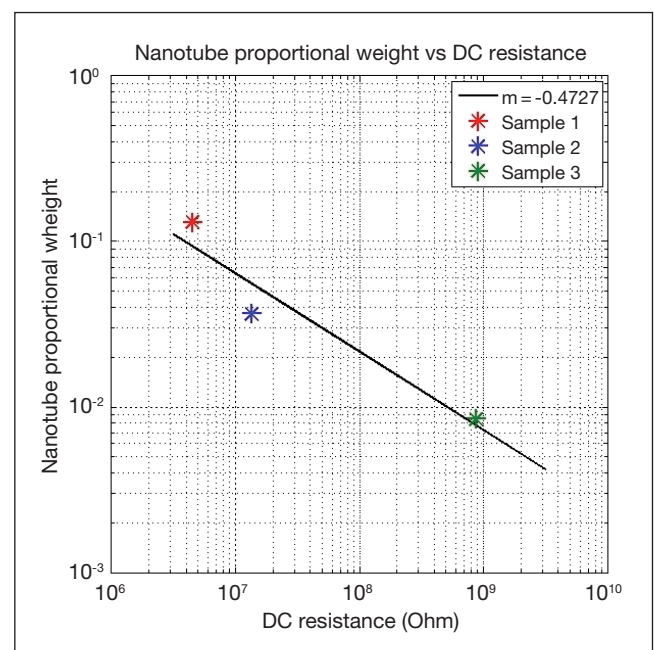

Figure 10. Correlation between the SWCNT weight proportion determined from TGA analysis and the DC resistance. As mentioned above, the DC resistance for a dense thin film is lower than for a light one.
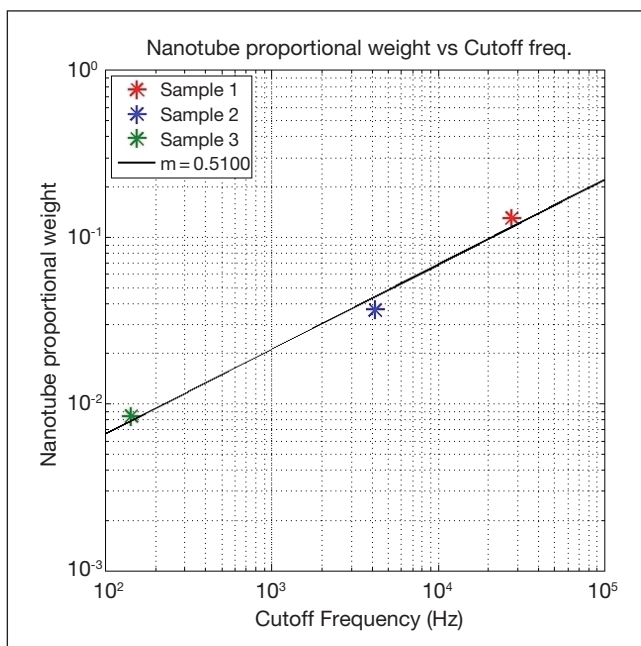
Figure 11. Correlation between the SWCNT weight proportion determined from TGA analysis and the cutoff frequency. For a sample with more tubes in the network, the distance between tube junctions is lower than in a sample with fewer tubes. Thus, the cutoff frequency for a dense sample is higher than the cutoff for a lighter sample.

Figure 12. Correlation between the SWCNT weight proportion determined from our method and optical absorption.

S_{22}, is not sensitive to doping or to any other chemical environment of the sample. After subtracting the background, due to the presence of carbonaceous products (fullerenes, amorphous carbon and graphitic particles) the intensity of this peak should be proportional to the amount of nanotubes. In fact, the S_{22} intensity is only able to yield the nanotube concentration that is relative to a known or standard concentration of CNTs [35].

In our samples, all the CNTs were obtained using the same method and came from the same batch. It can be assumed that the degree of impurities and carbonaceous products was the same. Therefore, as we were only interested in the relative amount of CNTs, a reference was not necessary. We used this method in order to validate the number of CNTs that was determined from the TGA using our method. The agreement is good [33], which means that our TGA analysis is reliable, as shown in Figure 12.

3. pH sensors

3.1. Experimental
Very thin (from around 100 to 150 nm) randomly oriented CNT networks, near their percolation threshold, were deposited on a transparent substrate: glass, quartz or plastic (PVC). The nanotubes were single-walled carbon nanotubes (SWNTs) grown using the HiPco process, which is supplied by the CNI. After they had been prepared in a light suspension (<1% in volume) in SDS (sodium dodecyl sulphate), they were sprayed onto the substrate using an airbrush. Once it had dried, the sample was submerged and shaken in pure water in order to remove the SDS. The resistances of the resulting CNTs networks ranged from 0.5 to 5 kohm, which is sufficient for their use as elec-
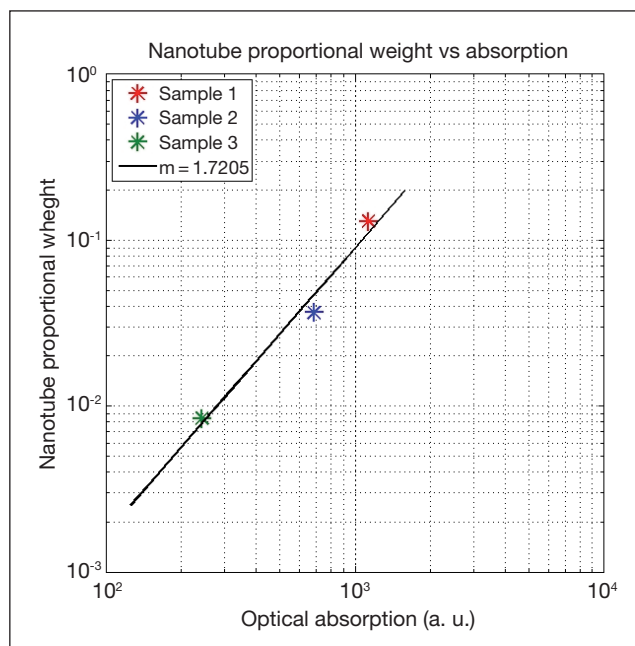
trodes in electrochemical cells. Some samples (CNT/SOCl$_2$) were made with previously functionalised CNT using SOCl$_2$ suspended in chlorobenzene. Once the CNT or CNT/SOCl$_2$ samples were dry, we used them as working electrodes to deposit the conducting polymer — polyaniline (PA) or polypyrrole(PPy) — on them electrochemically [37].

The electrochemical deposition was carried out galvanostatically using a Jaissle IMP 83 PC potentiostat. The carbon nanotubes with polyaniline (CNT/PA) were grown from an aqueous solution, 1M H$_2$SO$_4$, and 0.1M aniline in which the potential was controlled against an SCE reference electrode, as it is well known that only values in the 400<V<750mV range would give rise to the conductive emeraldine form [38]. Polypyrrole was grown from acetonitrile with 0.1M pyrrole, 0.2M LiClO$_4$ and 1% H$_2$O, as described in [39-40]. The resulting samples can be seen in Figure 13.

3.1.1. Raman characterisation
Raman spectroscopy was conducted using a microscope laser Raman spectrometer (Jobin Yvon) at a wavelength of 632.82-nm.

Raman spectra are very sensitive to the possible interactions between the CNT and the polymer [41-43]. Figure 14 shows the Raman spectra obtained on thin networks of carbon nanotubes with polyaniline a), CNT/PA films, compared to b) thin networks of CNT, showing the Raman characteristic lines of carbon nanotubes. The breathing mode is very visible for all samples, and the characteristic CNT lines are hardly modified. Due to PA, many lines appear on the CNT/PA, which can be identified as the conducting emeraldine form [38]. Similar result were obtained on CNT/PPy networks: for thin films, the Raman spectra show a superposition of CNT and PPy lines whereas when increasing the polypyrrole amount, the CNT breathing mode is hidden and the PPy lines are more visible [44].
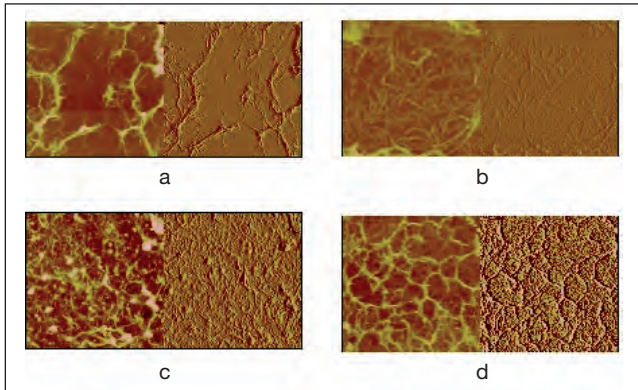
Figure 13. AFM images of a) a transparent CNT network on glass; the AFM square width is 15.0μm; b) a network of CNT/PA on quartz; sq. width 5.0μm; c) CNT/PPy: a PTS network on glass; electrodepositing time 33 min, density current j=0.08 mA/cm^2, sq. width 15.0μm; d) CNT/PPy: a PF6 network on glass; electrodepositing time 12min. min,density current j= 0,05 mA/cm^2, sq. width 5.0μm.

3.1.2. pH sensitivity: characterisation

Various buffer solutions were prepared that ranged from pH 1 to 13. The pH values of all the buffer solutions were controlled using a commercial pH sensor (Metrohm 744 pH meter, Germany). We measured the open circuit potential versus a saturated calomel electrode (SCE) when the CNT/PPy or the CNT/Pani was dipped into the buffer solution using a potentiometer (Jaissle, model PC IMP 83 PC). Before each measurement, the sensor was immersed in pure water in order to ensure the same starting conditions. Optical spectra were recorded using a double beam UV/VIS spectrometer (Perkin-Elmer, model Lambda 2).

Figure 15 shows the pH dependence of CNT/PPy (left) and CNT/Pani (right) on a transparent and flexible PVC substrate: both show a good linearity with slight hysteresis. For CNT/Pani, the slope is higher and close to the ideal Nernstian slope [45]. The graphs also show that the behaviour of pure CNT networks is pH dependent, but with a lack of linearity. The response time and stability is very good for both devices in all buffer solutions. The signal stabilizes in a few seconds and it remains stable for more than 5 min. In both cases we check the reproducibility, dipping the sensor in buffer solutions of
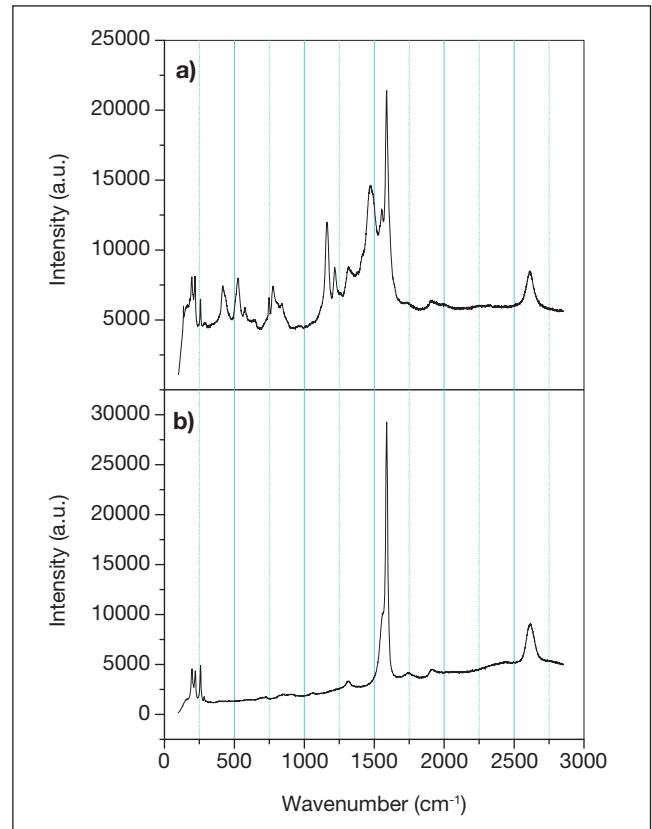

Figure 14. Raman spectra of thin networks of : a) carbon nanotubes with polyaniline, CNT-PA films; compared to b) thin networks of CNT, showing the Raman characteristic lines of carbon nanotubes.

pH 1 to pH 13 different times, obtaining a reproducible pH response.

It is well known that the colour of Pani changes with pH [38]. We analysed the pH dependence of the optical sensor CNT/Pani on a transparent substrate: optical spectra were recorded after the sample had been immersed in the corresponding buffer solution. The sample was blown dry in an argon stream but not washed in order to maintain the pH value in the thin film [37].

Figure 16 shows the UV/VIS spectra of CNT/Pani devices for the extreme values pH = 1 and pH = 13. It can be observed
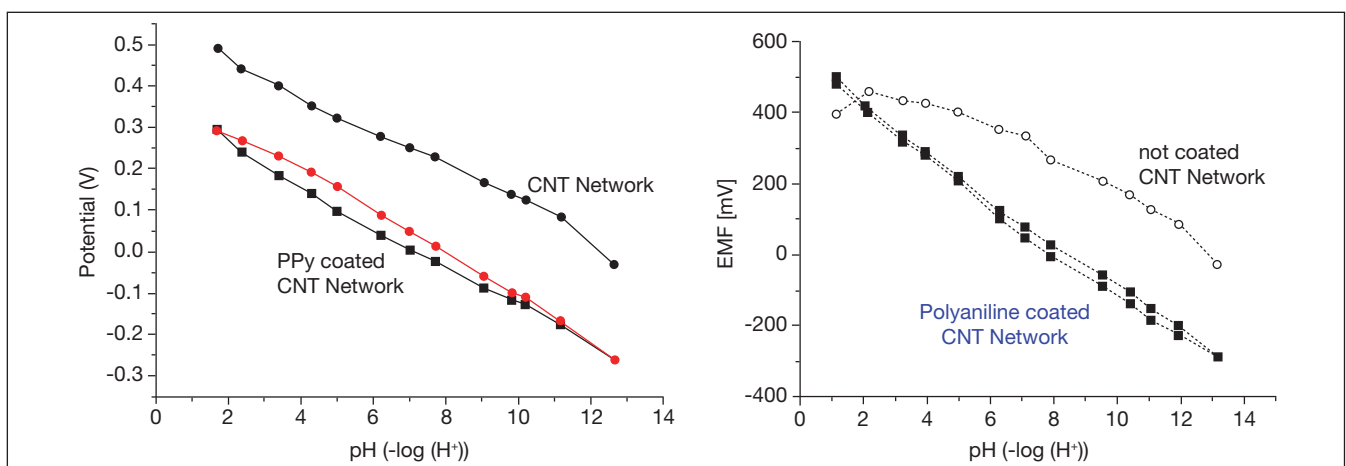

Figure 15: Left: pH dependence of the open circuit potential of a CNT/PPy sensor on a PVC substrate (in black pH=1→pH=13; in red pH=13→pH=1), in comparison to a pure CNT network on the same substrate (pH = 1 → pH = 13). Right: pH dependence of the open circuit potential of a CNT/Pani sensor on a PVC substrate (squares) in comparison to a pure CNT network (circles).
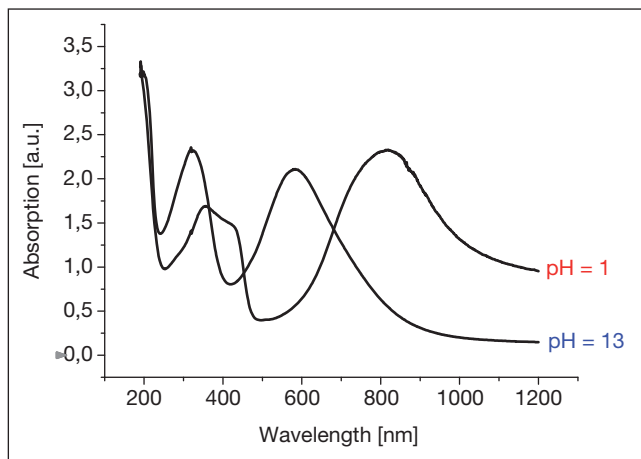
Figure 16. Optical pH response of CNT/Pani: we can see that the optical absorption UV/VIS spectra are totally different at pH 1 and pH 13, as the electronic energy levels of Pani are pH dependent.
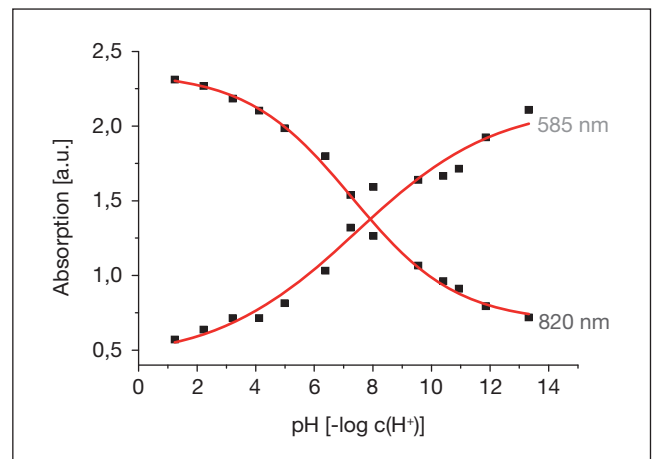

Figure 17. Optical pH response of CNT/Pani: both the absorption and the colour change with pH. It could be used as a sensor just by the colour changes

Table 1. Resistance per square R_{sq}, Electrical conductivity σ (calculated as having an estimated thickness of 150 nm) and transparency (Transmission, %T) of carbon nanotube (CNT), carbon nanotube-polyaniline (CNT-PA) and carbon nanotube-polypyrrole (CNT-PPy) thin films, with polypyrrole, obtained with different parameters: density current j and deposition time t.

	CNT	CNT/PA	CNT/PPy	CNT/PPy	CNT/PPy
j (mA/cm$^{2)}$	-		0.6	1.0	0.24
t (min)	-	20 - 45	6	7	10
R_{sq} (kΩ)	6.6	2.5	1.1—7	1.5—10	1.5—10
σ (S cm^{-1})	4 - 20	40 - 60	10 - 60	7 - 44	7 - 43
%T	80 - 90	62 - 90	75	45 - 75	75 - 83

that the spectra are pH-dependent. Figure 17 shows the transmittance at two different wavelengths over the whole pH range: we see a clear pH response, even if an almost linear optical response is only obtained for pH values ranging from pH 4 to 10.

The measurements that show the performance of different thin films studied [44] are summarised in Table 1.

4. Conclusions

Thin CNT networks can be deposited on a transparent substrate (glass, quartz or a flexible plastic), which results in a film that is electrically conducting, transparent and flexible. It is therefore possible to use these thin films as electrodes for a wide range of applications in which transparency, flexibility and conductance are required. A method for determining the number of nanotubes deposited in a sample was also developed and tested.

Carbon nanotube thin films can be used to electrochemically grow conducting polymers on them. We were thus able to build a solid state pH sensor by depositing polypyrrole or polyaniline on single-walled CNT networks.

We show that CNT/polypyrrole and CNT/polyaniline can be used as solid state pH sensors: their response is linear, fast and reproducible. Compared with pure CNT networks, the linearity

and stability are improved. The transparent CNT/Pani devices could be used as optical sensors, since their colour changes considerably as the pH level changes, although not linearly.

Finally, our results show that any defined substrate, of any shape, on any surface, may be converted into a flexible electrode depositing on it carbon nanotubes. It could be transformed into a solid state sensor by using thin film CNT networks and conducting polymers.

References

[1]   Iijima S. (1991). *Nature* 354:56
[2]   Saito R., Dresselhaus G., Dresselhaus M.S. (2003). „*Physical Proprieties of Carbon Nanotubes",* Imperial College Press
[3]   Reich S., Thomsen C., Maultzsch J. (2003). *Carbon Nanotubes: basic concepts and physical properties,* Wiley-VCH.
[4]   Saito R., Dresselhaus G., Dresselhaus M.S., Jorio A. (2005). *Phys. Rep.* 409:47
[5]   Vohrer U., Kolaric I., Haque M.H., Roth S., Detlaff-Weglikowska U. (2004). *Carbon* 42:1159
[6]   Zhao J.J., Chen X.S., Xie J.R.H. (2006). *Anal. Chem. Acta* 568:161
[7]   Huh Y., Lee J.Y., Lee C.J. (2005).*Thin Solid Films* 475:267
[8]   Snow E.S., Perkins F.K., Houser E.J., Badescu S.C., Reinecke T.L. (2005). *Science* 307:1942
[9]   Raffaelle R.P., Landi B.J., Harris J.D., Bailey S.G., Hepp A.F. (2005). *Materials Science and Engineering* B, 116, 3:233
[10] Duesberg G.S., Graham A.P., Liebau M., Seidel R., Unger E., Kreupl F., Hoenlein W. (2003). *Nano Lett.* 3, 2:257
[11] Sharma P., Ahuja P. (2008). *Materials Research Bulletin* 43, 10:2517
[12] Lee J.S., Chandrashekar A., Parikh K., Cattanach K., Manohar S.K., Lee G.S., Overzet L. (2005). *Solid-State Sensors, Actuators and Microsystems* 2:1943
[13] Artukovic E., Kaempgen M., Hecht D., Roth S., Grüner G. (2005). *Nano Lett*. 5, 4:757

[14] Kaempgen M., Duesberg G.S., Roth S. (2005). *Appl. Surf. Sci.* 252, 12:425

[15] Ryan K. P., Cadek M., Nicolosi V., Blond D., Ruether M., Armstrong G., Swan H., Fonseca A., Nagy J.B., Maser W., Blau W., Coleman J. (2007). *Composites Science and Technology* 67, 7-8:1640

[16] Sanchez Arribas A., Bermejo E., Chicharro M., Zapardiel A., Luque G., Ferreyra N., Rivas G.A. (2006). *Analytica Chemica Acta* 577, 2:183

[17] Huang H., Zhang W.K., Gan X.P., Wang C., Zhang L. (2007). *Materials Letters* 61, 1:296

[18] Gupta V., Miura N. (2006). *Journal of Power Sources* 157, 1:616

[19] Maiti A. *Microelectronics Journal*, 39, 2:208 (2005).

[20] Utriainen M., Karpanoja E., Paakkanen H. (2003). *Sens. Actuators* B 93:17

[21] Collins P.G., Bradley K., Ishigami M., Zettl A. (2002). *Science* 287:1801

[22] Kaempgen M., Roth S. (2006). *J. Electroanal. Chem.* 586:72

[23] Ionescu R., Llobet E., Al-Khalifa S., Gardner J.W., Vilanova X., Brezmes J., Correig X. (2003). *Sens. Actuators* B 95:203

[24] Ferrer-Anglada N., Kaempgen M., Dettlaff-Weglikovska U., Skákalová V., Roth S. (2004). *Diamond and Rel. Mat.* 13:156

[25] Wu Z., Chen Z., Du X., Logan J., Rinzler A.G. et al. (2004). *Science* 305:1273

[26] Yan H., Cannon W.R., Shanefield D.J. (1998). *Ceramics Int.* 24:433

[27] Parekh B., Fanchini G., Eda G., Chhowalla M. (2007). *Appl. Phys. Lett.* 90:121913

[28] Skákalová V., Kaiser A.B., Woo Y.-S., Roth S. (2006). *Phys. Rev.* B 74:085403

[29] Burke P.J. (2004). *Solid-State Electronics* 48, 10-11:1981

[30] Xu H., Zhang S., Anlage S.M., Hu L., Grüner G. (2008). *Phys. Rev.* B 77:075418

[31] Landau L.D., Levich B.G. (1942). *Acta Physiochim.*, URSS, 17:42-54

[32] Yan H., Cannon W.R., and Shanefield D.J. (1998). *Ceramics Int.* 24:433

[33] Pérez-Puigdemont J., Ferrer-Anglada N. (2008). *Phys. Stat. Sol.* (b) 245, No. 10

[34] Xu H., Anlage S.M., Hu L., Grüner G. (2007). *Appl. Phys. Letters* 90, 1:83119

[35] Itkis M.E., Perea D.E., Niyogi S., Rickard S.M., Hamon M.A., Hu H., Zhao B., Haddon R.C. (2003). *Nano Letters* 3:309

[36] Jost O., Gorbunov A.A., Pompe W., Pichler T., Friedlein R., Knupfer M., Reibold M., Bauer H.D., Dunsch L., Golden M.S., Fink J. (1999). *Appl. Phys. Lett.* 75:2217

[37] Ferrer-Anglada N., Kaempgen M., Roth S. (2006). *Phys. Stat. Sol.* (b)13:3519

[38] Pron A., Lefrant S. In: Nalva H.S. (Ed.). *Handbook of Organic Conductive Molecules and Polymers*, vol. 3, Wiley, 1997, pp. 183-215

[39] Ribó J.M., Dicko A., Vallés M.A. et al. (1993). *Polymer* 34 (5) 1047

[40] Gomis V., Ferrer-Anglada N., Movaghar B., Ribó J.M., El-Hachemi Z., Jhang S.H. (2003). *Phys. Rev.* B 68 115208.1-115208.5

[41] Cochet M., Maser W.K., Benito A.M. et al. (2001). *Chem. Commun.* 16:1450

[42] Cochet M., Buisson J.P., Weáry J., Jonusauskas G., Faulques E., Lefrant S. (2001). *Synth. Met.* 119:389

[43] Dettlaff-Weglikowska U., Skaákalová V., Benoit J.-M., Graupner R. In: Kuzmany H., Fink J., Mehring M., Roth S. (Eds.). *Molecular Nanostructures: XVII Int. Winterschool/Euroconference on Electronic Properties of Novel Materials*, 2003, AIP Conf. Proceedings, p. 273.

[44] Ferrer-Anglada N., Gomis V., El-Hachemi Z., Kaempgen M., Roth S. In: Kuzmany H., Fink J., Mehring M., Roth S. (Eds.). *Electronic Properties of Synthetic Nanostructures: XVIII Int. Winterschool/Euroconference on Electronic Properties of Novel Materials*, 2004, AIP Conf. Proceedings, p. 591.

[45] Karyakin A.A., Vuki M., Lukachova M.V., Karyakina E.E., Orlov A.V., Karpachova G. P., Wang J. (1999). *Anal. Chem.* 71:2534

About the authors

Jordi Pérez-Puigdemont is a student of Engineering of Telecommunications in Barcelona, and of the Master of Photonic Sciences of the Universitat Politècnica de Catalunya. *A big part of the presented work is part of his Final Project of Career, which it will soon present.*

Nuria Ferrer-Anglada is a full professor in the Department of Applied Physics of the Universitat Politècnica de Catalunya. *Her research is in the field of the new materials for electronic devices, using carbon nanotubes in particular as* *a constituent in nanocompounds. The collaboration with the group of the Max-Planck-Institut for the Research in Solid Materials of Stuttgart is already 10 years of seniority.*

Bernat Terrés is a student of Engineering of Telecommunications in Barcelona, to the Universitat Politècnica de Catalunya. *His contribution to the work, carried out partly in the Max-Planck-Institut of Stuttgart under the direction of S. Roth, has been part of his Final Project of Career, presented in November of 2008.*

Martti Kaempgen has a degree in chemistry and at present is a researcher *at the School of Materials Science and Engineering, Nanyang Technological University, Singapore. He made his Doctoral Thesis at the MPI of Stuttgart and a Postdoctoral research stay at the Department of Physics of the University of California (UCLA), Los Angeles, USA.*

Siegmar Roth is researcher and head of research in the MPI of Stuttgart, where he directs a group of about 20 persons and different european projects, about different applications of the carbon nanotubes. He is also a head of research of the company SINEUROP Nanotech of Stuttgart.